Experimental Thermal and Fluid Science 48 (2013) 147–155

Contents lists available at SciVerse ScienceDirect

Experimental Thermal and Fluid Science

journal homepage: www.elsevier.com/locate/etfs

Effects of upwind area of tube inserts on heat transfer and flow resistance characteristics of turbulent flow

Jian Guo [a], Yuexiang Yan [b], Wei Liu [b], Fangming Jiang [a,*], Aiwu Fan [b,*]

[a] Laboratory of Advanced Energy Systems, CAS Key Laboratory of Renewable Energy and Gas Hydrate, Guangzhou Institute of Energy Conversion, Chinese Academy of Sciences (CAS), Guangzhou 510640, China

[b] School of Energy and Power Engineering, Huazhong University of Science and Technology, Wuhan 430074, China

ARTICLE INFO

Article history:
Received 22 November 2012
Received in revised form 23 January 2013
Accepted 18 February 2013
Available online 5 March 2013

Keywords:
Upwind area
Heat transfer
Flow resistance
Enhanced tube
Conical-strip insert
Turbulent flow

ABSTRACT

Effects of reducing the upwind area of conical-strip tube inserts on heat transfer and friction factor characteristics of turbulent flow are experimentally investigated. The conical-strip insert resembles one quarter of the conical-ring insert in terms of its upwind area. Results show that the Nusselt number for the case with conical-strip inserts is only 53–56% of that for the case with conical-ring inserts, the friction factor for the former is merely 4–6% of that for the latter, and thus the thermo-hydraulic performance factor can be enhanced by 36–61% if replacing conical-ring inserts with conical-strip inserts for turbulent flow within *Re* range 5000–25,000. In addition, a comparative study of the short conical strip and the T-type conical strip, which can be regarded as boundary-cutting and core-cutting to the normal conical strip respectively, is performed. Results indicate that the flow resistance can be reduced by both methods. However, a weakened heat transfer and a worsened thermo-hydraulic performance are obtained for the case with boundary-cutting strip inserts. In contrast, the case with T-type core-cutting conical-strip inserts, if a suitable core-cutting size is taken, shows a better thermo-hydraulic performance as compared with the case with normal conical-strip inserts when the Reynolds number is relatively large. Effects of the pitch between neighboring strips have also been examined. It is found that smaller pitch leads to higher heat transfer rate whereas the flow resistance is increased. A moderate pitch between conical strips is beneficial to the overall thermo-hydraulic performance.

© 2013 Elsevier Inc. All rights reserved.

1. Introduction

Heat transfer augmentations are frequently encountered in many industrial fields like power generation, air-conditioning, petrochemical engineering. Researchers throughout the world have made great efforts to develop various heat transfer augmentation techniques [1–3], classified distinctly into two categories: passive and active. The passive technique, due to no consumption of any additional energy, is generally more popular in practice. Utilizations of various kinds of tube inserts, such as twisted tape [4–6], helical screwed tape [7,8], coiled wire [9–11], louvered strip [12], porous media insert [13,14], and conical rings [15–18], are typical representatives of the passive technique. Tube inserts activate and intensify the swirl flow in the tube, reducing the thickness of the thermal boundary layer. However, the flow resistance is also increased as the tube inserts reduce the cross-sectional area of fluid pathway.

Researching and optimizing the thermo-hydraulic performance of tube flow with tube inserts has gained continuing attentions in related scientific and industrial fields. The purpose is to seek for a maximized heat transfer augmentation with flow resistance being controlled as low as possible. Saha et al. [19,20] experimentally studied the heat transfer and friction factor characteristics of laminar flow in a circular tube fitted with regularly spaced twisted tape elements, which less block the fluid flow compared with the continuous twisted tape. Their experimental results showed that the pressure drop for the flow in tube inserted with segmented twisted tape elements is 40% smaller than that for the flow in tube inserted with continuous twisted tape, and the former has a better thermo-hydraulic performance than the latter. Eiamsa-ard et al. [21] experimentally investigated the convective heat transfer behaviors for both laminar and turbulent flow in a circular tube fitted with the segmented twisted tape elements, and got similar observations as reported by Saha et al. [19,20].

Further, Ayub and Al-Fahed [22] experimentally studied the effects of upwind area of the twisted tape. Results showed that enlarging the gap between the tape edge and the tube wall by

* Corresponding authors. Address: 2 Nengyuan Rd., Wushan, Tianhe District, Guangzhou 510640, China. Tel./fax: +86 20 87057656 (F. Jiang), tel.: +86 27 87542618; fax: +86 27 87540724 (A. Fan).

E-mail addresses: jiangfm@ms.giec.ac.cn (F. Jiang), faw@mail.hust.edu.cn (A. Fan).

0894-1777/$ - see front matter © 2013 Elsevier Inc. All rights reserved.
http://dx.doi.org/10.1016/j.expthermflusci.2013.02.017

Nomenclature

c_p	specific heat at constant pressure, J kg^{-1} K^{-1}
D	the tube diameter, m
f	friction factor
h	heat transfer coefficient, W m^{-2} K^{-1}
k	thermal conductivity, W m^{-1} K^{-1}
L	length of the test tube, m
L_c	radius of core-cutting, m
L_s	length of the conical strip, m
Nu	Nusselt number
Pr	Prandtl number
Δp	pressure drop, N m^{-2}
Q	heat transfer rate, J s^{-1}
Re	Reynolds number
r	dimensionless length of the conical strip, $r = L_s \sin \alpha/(D_i/2)$
r_c	dimensionless radius of core-cutting, $r_c = L_c \sin \alpha/(D_i/2)$
S	pitch of the conical strips, m
s	dimensionless pitch of the conical strips, $s = S/D_i$
T	temperature, K
ΔT	temperature difference, K
U	flow velocity, m s^{-1}
V	volume flow rate, m^3 s^{-1}

Greek symbols

α	slant angle (°)
ν	kinetic viscosity, m^2 s^{-1}
ρ	fluid density, kg m^{-3}
π	circumference ratio

Subscripts

0	plain tube
i	inner
in	inlet of the tube
o	outer
out	outlet of the tube
w	tube wall

decreasing the width of twisted tape could effectively reduce the friction factor. Eiamsa-ard et al. [23] numerically studied the convective heat transfer behaviors in the tube fitted with narrow twisted tapes. They also found that it was beneficial to reducing the pressure flow resistance if decreasing the width of twisted tape insert. However, both the heat transfer and the thermo-hydraulic performance were weakened. Guo et al. [24] investigated the heat transfer and friction factor characteristics in the tube fitted with

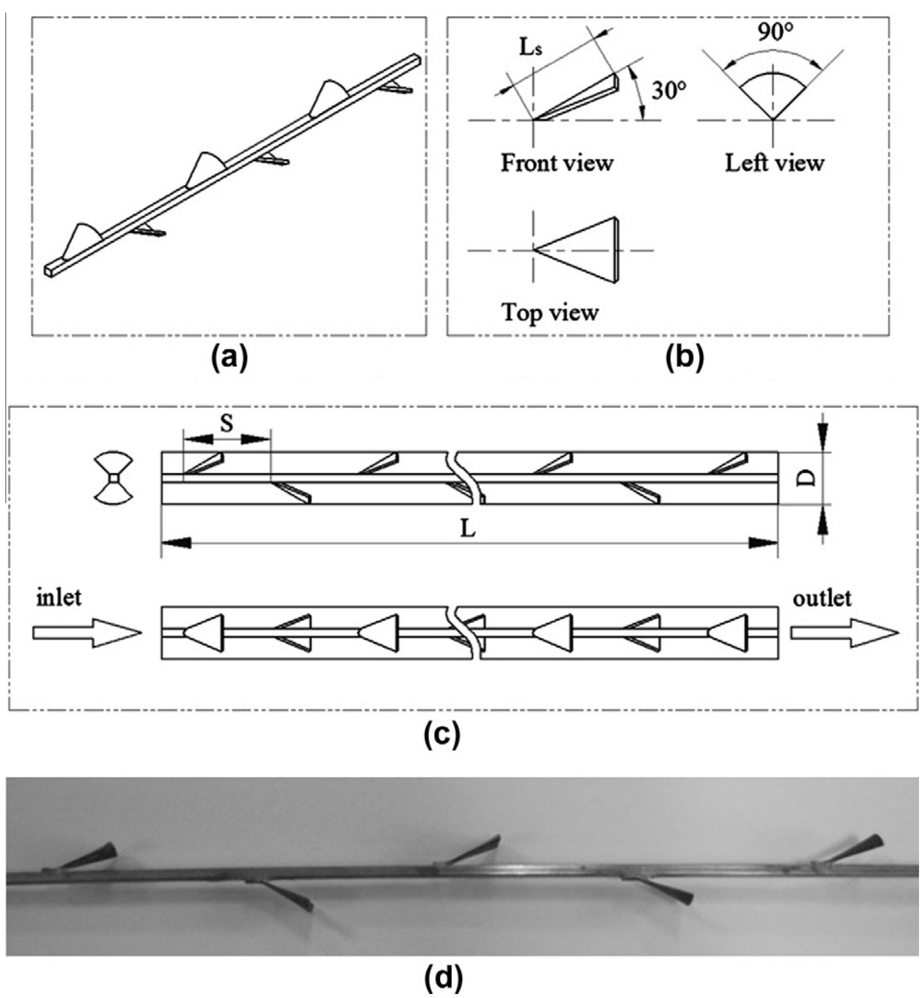

Fig. 1. (a) Schematic of the conical-strip insert, (b) geometry of the conical strip, (c) schematic of the circular tube with the conical-strip insert, and (d) picture of the conical-strip insert.

center-cleared twisted tapes. Unlike the narrow twisted tape whose upwind area is reduced by cutting off the tape edge near the tube wall, the center-cleared twisted tape cuts off the tape portion in the core flow region. It was found that this method is capable of reducing the flow resistance and maintaining a high heat transfer performance at the same time. Therefore, the thermo-hydraulic performance was enhanced.

Although tremendous efforts have been made to reduce the flow resistance by the method of decreasing the area of the tube insert, the research focused on decreasing the upwind area by cutting off the insert portion in the core flow region is very rare to date. The present work chooses the conical-strip insert and designs experiments to study the effects of reducing the upwind area of the tube insert. The conical-strip insert is a modification of the conical rings [25,26]. Experimental studies by Promvonge [17] found that the conical-ring insert is a good device for heat transfer augmentation, whereas a substantial increment of flow resistance is also accompanied due to the large upwind area of the conical ring, which severely blocks the flow path. In contrast to the conical ring, the conical strip brings less blocking effect to the flow in the core flow region. It is thus expected that the conical-strip insert can reduce the flow resistance and at the same time keep strong enough disturbance to the thermal boundary layer. This work will investigate the heat transfer and friction factor characteristics of turbulent flow in circular tubes fitted with various conical-strip

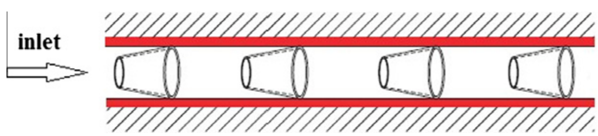

Fig. 2. Sketch of the tube with conical rings.

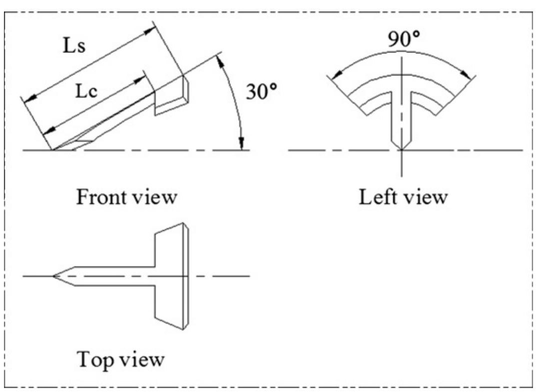

Fig. 3. Geometry of the T-type conical strip.

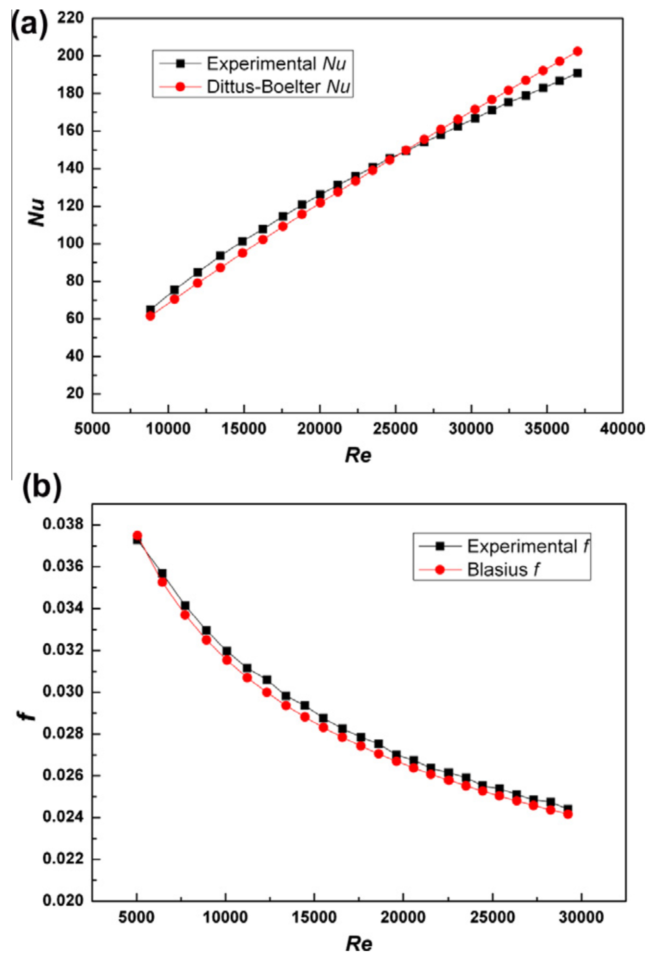

Fig. 5. The Nusselt number (*Nu*) and friction factor (*f*) versus the Reynolds number (*Re*) for turbulent flow in smooth: (a) *Nu* and (b) *f*.

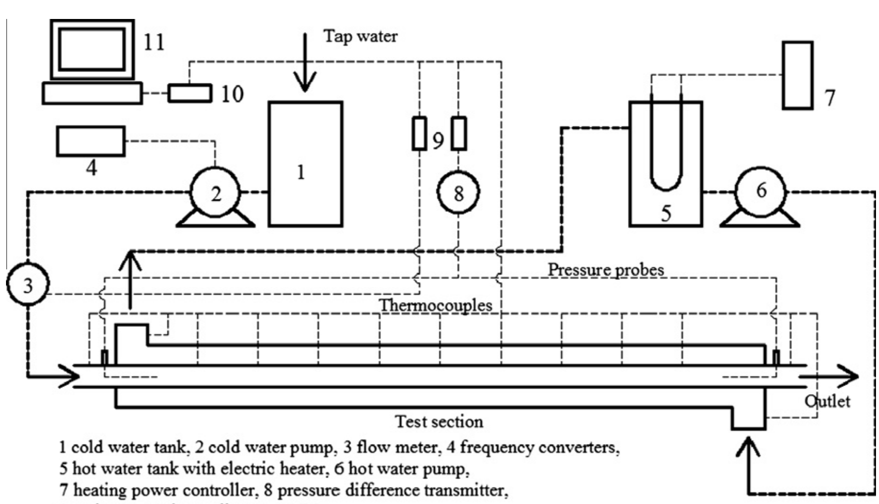

Fig. 4. Schematic of the experimental apparatus.

inserts of different geometrical parameters. Comparisons will be made between the effects of removing away the portions of the conical strip near the tube wall and in the core flow region.

2. Details about the experiment

2.1. Geometry of the inserts

The geometry of the conical-strip insert is depicted in Fig. 1. For comparison, a sketch of the tube fitted with the conical rings [17] is also shown in Fig. 2. It is clearly seen that the conical strip resembles one quarter of the conical ring. With this modification, blocking to the flow path due to the inserts is largely reduced in the core flow region while remains relatively large in the vicinity of the boundary layer. In the present study, the inner diameter (D_i) and thickness of the tested tube are 18 mm and 2 mm, respectively. The strips with thickness of 1 mm are welded on a 3×3 mm square steel rod, with a slant angle of $\alpha = 30°$ and staggered array to give the best performance reported in [25,26]. To characterize the geometrical parameters of the conical strip, we defined two dimensionless variables, one is the dimensionless radius, $r = L_s \sin\alpha/(D_i/2)$, and the other is the dimensionless pitch, $s = S/D_i$. $r = 1$ means that the outer edge of conical strip with the length (L_s) of 15 mm reaches the tube wall. $r = 0.89$ means a reduction of the upwind area by cutting off the strip portion in the vicinity of boundary layer. In addition, we proposed a T-type conical strip, as depicted in Fig. 3. The T-type conical strip is a modification to the conical strip of $r = 1$ by cutting off the strip portion in the core flow region except a portion with width of 3 mm for fixing. And a dimensionless core-cutting radius, $r_c = L_c \sin\alpha/(D_i/2)$, has been defined.

2.2. Experimental apparatus

Experiments were conducted in a double-tube heat exchanger made of stainless steel. The schematic of the experimental apparatus is shown in Fig. 4. The length of the test section is 2000 mm. The outer tube is 42 mm in inner diameter and 3 mm thick, covered by a 60-mm thick thermal insulating layer. Cold water coming from a tank with a stable water level flows through the inner tube, and finally effuses the system. The volumetric flow rate is controlled by adjusting the frequency of the pump that drives the cold water flow. Hot water cycles between the outer tube and hot water tank. Temperature of the hot water is controlled by an electrical heater. A high flow rate of the hot water is adopted to obtain an approximately uniform wall temperature profile along the outer surface of the tube. By doing so, derivation of the heat transfer coefficient in the inner tube is simplified.

A differential gauge with an accuracy of ±5% is used to measure the pressure drop along the test section of the inner tube. The gauge's measuring range is 0–32 kPa. Four T-type thermocouples (accuracy: ±0.2 °C) are placed in four thermal wells (1 mm in inner diameter and 0.8 mm thick), which are immersed up to the middle of the tube to measure the inlet/outlet temperatures of both cold and hot water. In order to get the bulk temperature, metal wire meshes are installed as baffles before the thermal wells. Nine armored thermocouples with an accuracy of ±1% are installed with equal spacing on the outer surface of the inner tube to measure the wall temperature. A turbine flow meter is adopted to measure

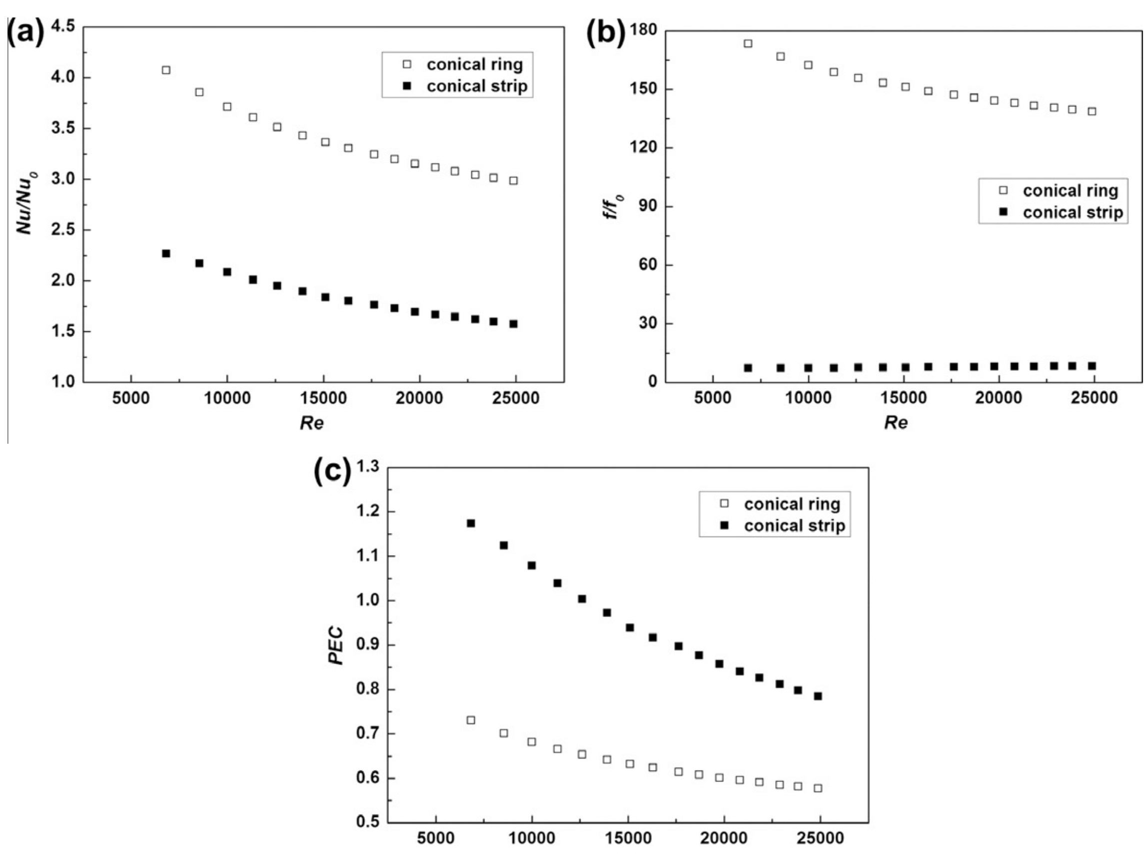

Fig. 6. Comparisons of the Nusselt number ratio (Nu/Nu_0), the friction factor ratio (f/f_0) and the thermal performance factor (PEC) for the conical-strip and conical-ring inserts: (a) Nu/Nu_0, (b) f/f_0, and (c) PEC.

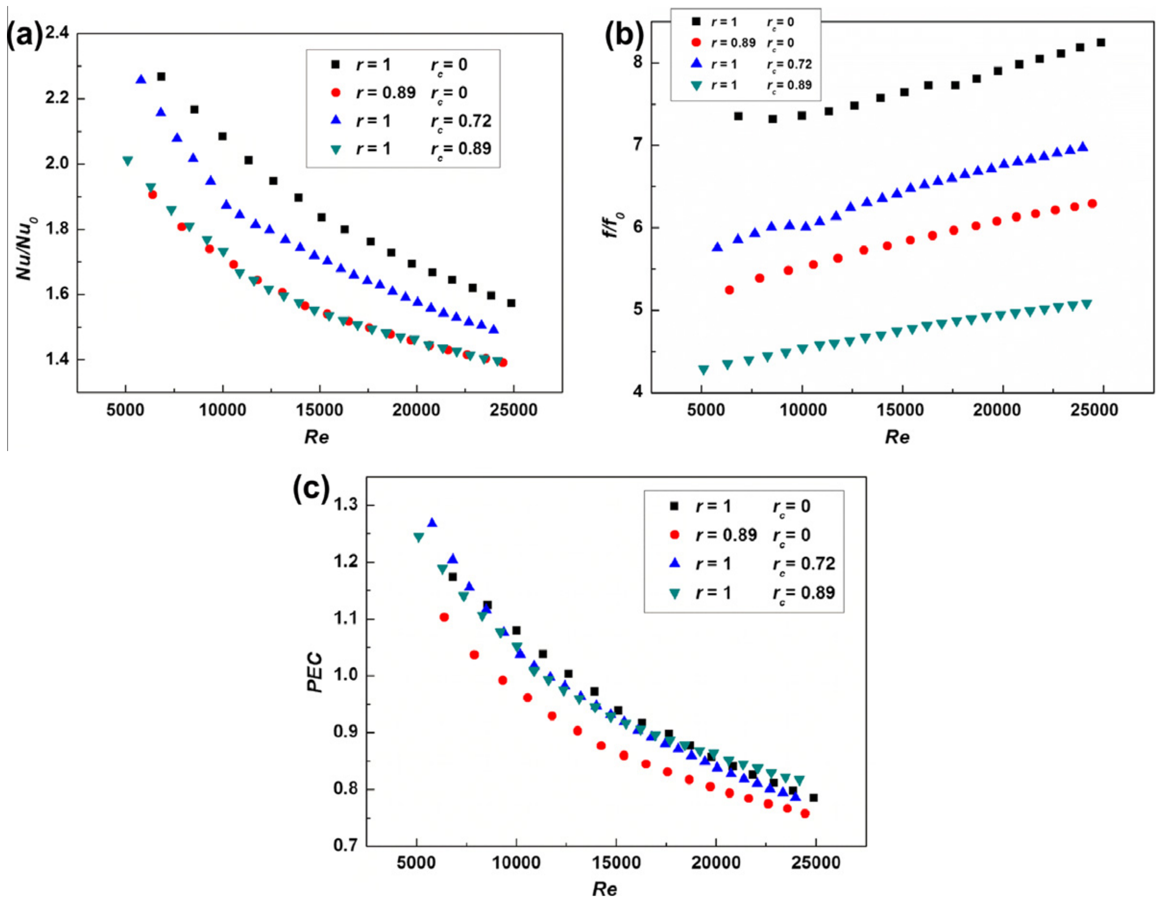

Fig. 7. The Nusselt number ratio (Nu/Nu_0), the friction factor ratio (f/f_0) and the thermal performance factor (*PEC*) versus the Reynolds number (*Re*) for conical-strip inserts with different upwind areas: (a) Nu/Nu_0, (b) f/f_0, and (c) *PEC*.

the volumetric flow rate of the cold water. Its measurement range is 0.15–1.5 m^3/h and has an accuracy of ±1%. A data acquisition system is used to collect and process all these measured signals.

2.3. Data processing

Unless otherwise stated, the thermo-physical and transport properties of the inner tube side are determined in terms of the average value of the inlet and outlet temperature, T_m, as defined in the following equation.

$$T_m = \frac{T_{in} + T_{out}}{2} \tag{1}$$

The average velocity in the test tube is calculated through Eq. (2), where V_{in} is the volumetric flow rate of the water at the inlet. Here, the subscript '*in*' or '*out*' denotes that the property is determined by the inlet or outlet temperature, respectively.

$$U_m = \frac{V_{in}\rho_{in}}{\pi D_i^2 \rho/4} \tag{2}$$

The Reynolds number and friction factor are calculated by:

$$Re = \frac{U_m D_i}{\nu} \tag{3}$$

$$f = \frac{\Delta p}{(\rho U_m^2/2)(L/D_i)} \tag{4}$$

The total heat transfer rate Q is calculated by,

$$Q = \rho_{in} c_p V_{in}(T_{out} - T_{in}) \tag{5}$$

The Nusselt number (*Nu*) can be calculated based on:

$$h = \frac{Q}{\pi D_i L \Delta T} \tag{6}$$

$$\Delta T = \frac{(T_w - T_{in}) - (T_w - T_{out})}{\ln\frac{T_w - T_{in}}{T_w - T_{out}}} \tag{7}$$

$$h_i = \frac{1}{\frac{1}{h} - \frac{D_i}{2k_w}\ln\frac{D_o}{D_i}} \tag{8}$$

$$Nu = \frac{h_i D_i}{k} \tag{9}$$

where h is the total heat exchange coefficient of the inner tube; D_o is the outer diameter of the inner tube; L is the length of the tested section; T_w is the average temperature of the outer surface of the inner tube; k_w is the thermal conductivity of the inner tube wall; k is the thermal conductivity of the cold water at T_m.

The experimental uncertainties were calculated following the Coleman and Steele method [27] and ANSI/ASME standard [28]. The maximum uncertainties of the Reynolds number, friction factor, and Nusselt number were analyzed to be about ±1.1%, ±5.4%, and ±5.1%, respectively. Detailed processes of the uncertainty calculations could be found in the appendix.

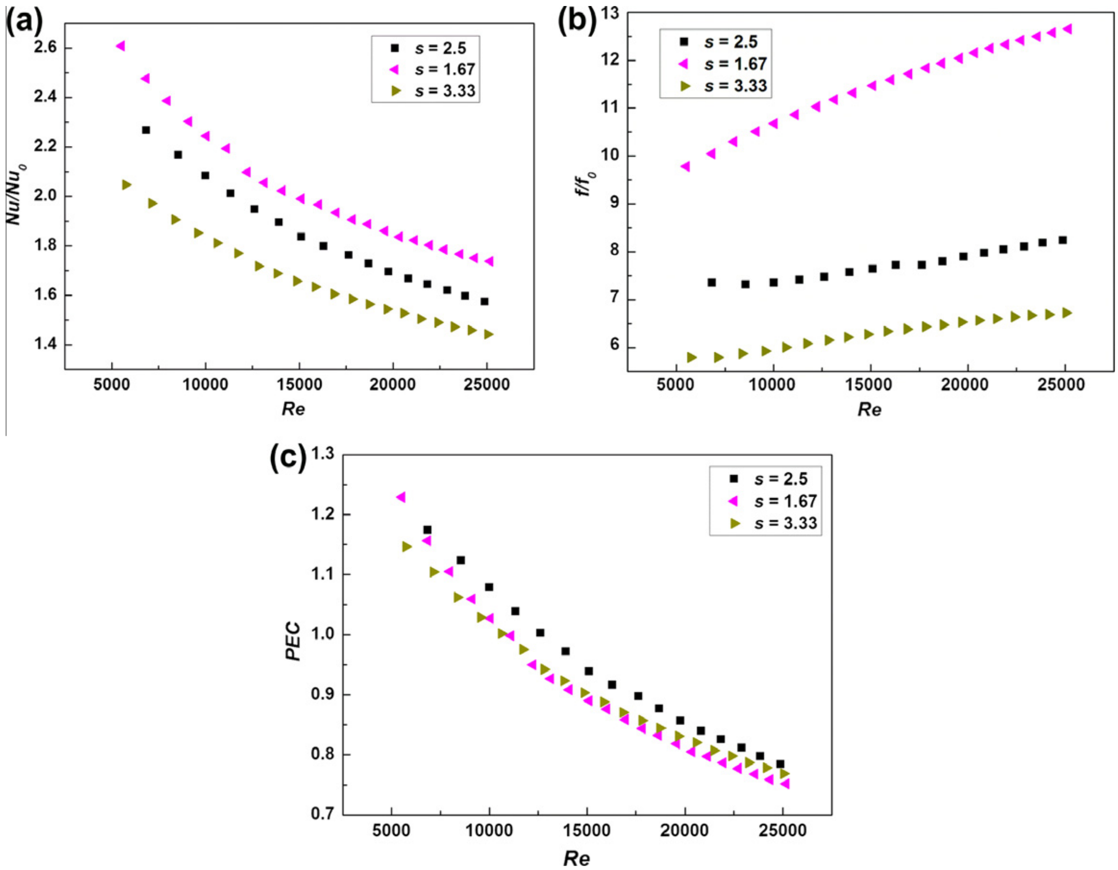

Fig. 8. The Nusselt number ratio (Nu/Nu_0), the friction factor ratio (f/f_0) and the thermal performance factor (*PEC*) versus the Reynolds number (*Re*) for conical-strip inserts with different pitches: (a) Nu/Nu_0, (b) f/f_0, and (c) *PEC*.

3. Results and discussions

3.1. Reliability validation

Before performing the experiments with respect to tube inserts, an experiment with respect to plain tube is conducted to verify the reliability of the experimental apparatus and data processing procedure. Fig. 5a and b shows the variation curves of the Nusselt number and friction factor as function of the Reynolds number, respectively. It can be seen from Fig. 5a that the experimental results of the Nusselt number agree well with the theoretical predictions of the Dittus–Boelter correlation (see Eq. (10)). The maximum deviation is less than 6%. From Fig. 5b it is noted that the experimental results of friction factor match satisfactorily with the values given by Blasius correlation (see Eq. (11)) and the maximum deviation is less than 5%.

$$Nu_0 = 0.023Re^{0.8}Pr^{0.4} \tag{10}$$

$$f_0 = 0.3164Re^{-0.25} \tag{11}$$

Both Eqs. (10) and (11) are used to describe fully developed tube flow. The tested tube flow has a uniform temperature distribution at the inlet. Though the flow-entrance effect may bring deviation at experimental results to the theoretical data calculated from Eqs. (10) and (11), it would be negligible as the flow is in turbulent regime and the test section is long enough to dilute the entrance effect. Data presented in Fig. 5 justified this. Hence, reliability of the experimental apparatus and data processing procedure are validated.

Correlations for both the Nusselt number and friction factor are created based on the experimental data from plain tube case, as described in Eqs. (12) and (13). The accuracies of Eqs. (12) and (13) are within ±4% and ±2%, respectively.

$$Nu_0 = 0.063Re^{0.7}Pr^{0.4} \tag{12}$$

$$f_0 = 0.3112Re^{-0.247} \tag{13}$$

Following we present first the results from the conical strip case and compare the data with those from conical ring case, then present and compare the results from the conical strip of $r = 1$, the boundary-cutting conical strip ($r = 0.89$) and the core-cutting conical strip ($r = 1$, $r_c = 0.72$, 0.89) cases, last investigate the effect of pitch between conical strips.

3.2. Comparisons of conical strip and conical ring cases

The ratios, Nu/Nu_0 and f/f_0 are adopted, respectively, to evaluate the heat transfer enhancement and the flow resistance increase for the tube flows. Nu_0 and f_0 are calculated from the empirical correlations of Eqs. (10) and (11), respectively. In order to evaluate the thermo-hydraulic performance of the tubes with inserts, the performance evaluation criterion (*PEC*) proposed by Webb [29] is employed in the present work, as defined in the following equation:

$$\mathrm{PEC} = \frac{Nu/Nu_0}{(f/f_0)^{1/3}} \tag{14}$$

Nu/Nu_0, f/f_0 and *PEC* versus the Reynolds number for the conical strip and conical ring cases are displayed in Fig. 6a–c respectively. The values of *Nu* and *f* for the conical ring case are calculated from empirical correlations reported in [17], and the geometrical parameters of the conical-strip insert were selected to give the best overall performance. Data points denoted by the solid black squares are experimental results from the conical strip case with $r = 1$ and $s = 2.5$. From Fig. 6a it can be seen that the values of Nu/Nu_0 for both the conical ring and conical strip cases decrease as the Reynolds number increases, which indicates that the heat transfer augmentation effects for both cases are becoming weak with the increasing of *Re*. The conical ring case shows a better heat transfer enhancement than the conical strip case. The Nu/Nu_0 for the conical ring case is 1.78–1.90 times as that for the conical strip case in the *Re* range 5000–25,000. This is an expected result as the conical ring has a larger upwind area and imposes more intensive disturbance to the flow than the conical strip. However, this better heat transfer augmentation is realized at the cost of much more increment at flow resistance. As indicated by Fig. 6b, the f/f_0 for the conical ring case is 16.8–23.6 times as that for the conical strip case. From Fig. 6c one can see that, the *PEC* value for the conical strip case is much higher (~1.36–1.61 times) than that for the conical ring case across the whole *Re* range examined. All these demonstrate that, replacing the conical-ring insert with the conical-strip insert is beneficial to the overall thermo-hydraulic performance of tube flow.

3.3. Results from boundary-cutting and core-cutting conical strip cases

Further, we reduce the upwind area of conical strip by cutting away a portion of the strip in distinct region near the tube wall or in the core flow to investigate the effect of upwind area. Additional experiments were performed with respect to cases of smaller conical-strip insert, $r = 0.89$, and of T-type conical-strip insert, $r = 1$, $r_c = 0.72$ or 0.89. The dimensionless pitch was fixed ($s = 2.5$) for all these cases.

The variation curves of Nu/Nu_0, f/f_0 and *PEC* against *Re* for these cases are summarized in Fig. 7a–c, respectively. Note that $r_c = 0$ refers to the normal conical strip that has no cutting-away portion as shown in Fig. 1. It is clearly seen from Fig. 7a that, the heat transfer performance for the case of $r = 1$, $r_c = 0$ is better than that for the case of $r = 0.89$, $r_c = 0$. There are two reasons responsible for this. First, the thermal boundary layer can be disturbed more intensively if the conical strips are larger. Second, the larger conical strips with outer edge in touch with the tube wall ($r = 1$) would bring a fin effect. Although the flow resistance for the case of $r = 1$, $r_c = 0$ is larger than that for $r = 0.89$, $r_c = 0$, as depicted in Fig. 7b, the former has a higher *PEC* value than the latter, as depicted in Fig. 7c, indicating it is unfavorable to the thermo-hydraulic performance if reducing the upwind area of the conical strips by simply lowering *r*.

It is also seen from Fig. 7 that for the T-type conical strip cases, the heat transfer rate and the friction factor are both lowered. Both the heat transfer rate and friction factor decrease with the increment of the core-cutting radius r_c. The overall performance exhibits a more complicated characteristic (see Fig. 7c) than the heat transfer performance and flow resistance. Both the *PEC* values for the cases of $r_c = 0.72$ and 0.89 are slightly larger than that for the case of $r_c = 0$ when the Reynolds number is relatively small. Then they both decline and become smaller than that for the case of $r_c = 0$ when *Re* rises up to 8000. For further increased *Re*, the *PEC* value for the case of $r_c = 0.72$ becomes the smallest among the three cases, while, the *PEC* value for the case of $r_c = 0.89$ surpasses that for the case of $r_c = 0$ again once *Re* is greater than 18,000. A suitable cutting-away of the conical strips can be beneficial to the overall performance when the Reynolds number is relatively large.

It is well know that the convective heat transfer for tube flow is enhanced by an insert owing to the disturbance to the flow and the reduction of the boundary layer thickness due to the insert. Therefore, setting an insert as close as possible to the tube wall would be very important to the heat transfer augmentation. Cutting off a portion of insert in the core flow region will not be too detrimental to the heat transfer augmentation, whereas it may largely reduce the flow resistance and thus enhance the overall thermo-hydraulic performance.

3.4. Effects of the pitch

In the above cases, the dimensionless pitches of all the inserts were fixed, $s = 2.5$. We additionally studied the effects of the pitch with respect to the conical-strip inserts of $r = 1$, $r_c = 0$. Cases of $s = 1.67$, 2.5 and 3.33 are considered.

The variation curves of Nu/Nu_0, f/f_0 and *PEC* versus the Reynolds number for the three cases are depicted in Fig. 8a–c, respectively. It is noted that, the value of Nu/Nu_0 increases with the decrease of the dimensionless pitch *s*. That is to say, a closer alignment of conical strips along the tube can obtain a better heat transfer enhancement. But the closer alignment of conical strips also leads to more increment at flow resistance. Across the whole range of *Re* examined, the *PEC* value for the case of $s = 2.5$ is larger than those for the cases of $s = 1.67$ and 3.33. Therefore, a moderate pitch between the strips is suggested for the practical utilizations.

3.5. Correlations based on experimental data

Correlations of the Nusselt number and friction factor developed for present results, for $Re = 5000$–25,000, $r = 0.89$ and 1, $r_c = 0$, 0.72 and 0.89, and $s = 1.67$, 2.5 and 3.33, are described as below:

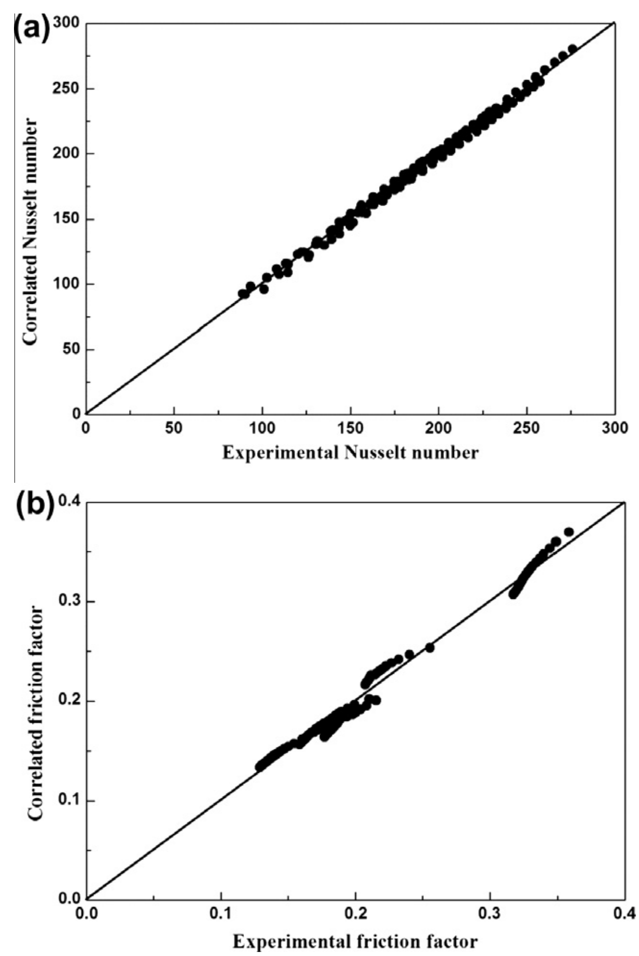

Fig. 9. Comparison of experimental results with the correlated values: (a) *Nu* and (b) *f*.

$$Nu_0 = 0.668Re^{0.537}Pr^{0.4}r^{1.29}(1-r_c)^{0.062}s^{-0.273} \tag{15}$$

$$f_0 = 1.66Re^{-0.123}r^{2.75}(1-r_c)^{0.221}s^{-0.87} \tag{16}$$

The correlation coefficients of the regressions are 0.98 and 0.97 for Eqs. (15) and (16), respectively. The correlated data of the Nusselt number and friction factor are compared with the experimental results, as displayed in Fig. 9a and b. The consistencies are within ±5% for the Nusselt number and ±7% for the friction factor.

4. Conclusions

Heat transfer, flow resistance and thermo-hydraulic performance of turbulent flow in a circular tube fitted with conical-strip inserts of various geometrical parameters have been investigated experimentally. The conical strip resembles one quarter of the conical ring in term of its upwind area. Experimental results show that the Nusselt number for the case with conical-strip insert is only 53–56% of that for the case with conical-ring insert, the friction factor for the former is merely 4–6% of that for the latter, and thus the thermo-hydraulic performance can be enhanced by 36–61% if replacing conical-ring inserts with conical-strip inserts. However, it may be improper to reduce the upwind area of a tube insert by cutting away its near-tube wall portion. A weakened heat transfer and a worsened thermo-hydraulic performance were found for the case with the conical-strip insert untouching the tube wall (r = 0.89) as compared with the case with the conical-strip insert in touch with the tube wall (r = 1). In contrast, cutting away the strip portion in the core flow region can be favorable to the thermo-hydraulic performance. It was found that the case with T-type conical-strip insert of r_c = 0.89 gave a higher *PEC* value as compared with the case with conical-strip insert without any portion being cut-away (r = 1) when Reynolds number was relatively large. In addition, effects of the pitch between the conical strips have been examined. Both the heat transfer and flow resistance were augmented when the dimensionless pitch s decreased. An optimized thermo-hydraulic performance was obtained at a moderate value of s, which found to be 2.5 found in the present study.

Acknowledgements

Financial supports from the Natural Science Foundation of China (Grants No. 51036003), the National Key Basic Research Development Program of China (2013CB228302) and the CAS "100 Talents" Program (FJ) are gratefully acknowledged.

Appendix A. The detailed calculations and analysis of the uncertainty

According to the Coleman and Steele method [27] and the ANSI/ASME standard [28], if a parameter R is a function of some measured parameters (Xi), then the uncertainty of R is affected by the individual uncertainties of Xi, and the absolute and relative uncertainties of R are calculated with the equations below:

$$\delta R = \left\{\sum_{i=1}^{N}\left(\frac{\partial R}{\partial X_i}\delta X_i\right)^2\right\}^{1/2} \tag{A1}$$

$$\frac{\delta R}{R} = \left\{\sum_{i=1}^{N}\left(\frac{\partial \ln R}{\partial X_i}\delta X_i\right)^2\right\}^{1/2} \tag{A2}$$

where δR and $(\delta R/R)$ represent the absolute and relative uncertainties, respectively.

Applying Eqs. (A1) to Eq. (1) (please refer to the manuscript), we can obtain the absolute uncertainties of T_m as below:

$$\delta T_m = \left(\left(\frac{1}{2}\delta T_{in}\right)^2 + \left(\frac{1}{2}\delta T_{out}\right)^2\right)^{1/2} \tag{A3}$$

where δT_{in} and δT_{out} are 0.2 °C based on the accuracy of the thermocouples, and thus δT_m = 0.14 °C. Similarly, the absolute uncertainties of T_w can be calculated as:

$$\delta T_w = \left\{\sum_{i=1}^{9}\left(\frac{1}{9}\delta T_i\right)^2\right\}^{1/2} = \left\{\sum_{i=1}^{9}\left(\frac{T_i}{9}\frac{\delta T_i}{T_i}\right)^2\right\}^{1/2} \tag{A4}$$

where T_i is each temperature measured by the nine armored thermocouples, and $\delta T_i/T_i$ is 1% based on their accuracies. The maximum δT_w is found to be 0.21 °C.

In present work, the physical property parameters, such as ρ, k, ρ_{in}, c_p, and v, are calculated using the linear formula:

$$Y = Y_a + \frac{Y_b - Y_a}{T_b - T_a}(T - T_a) \tag{A5}$$

where Y represents the physical property parameter, T is the temperature at which Y is to be evaluated, Y_a and Y_b are the known parameters corresponding to T_a and T_b, respectively. Then, the absolute uncertainties of the physical parameters can be calculated as:

$$\delta Y = \left|\frac{Y_b - Y_a}{T_b - T_a}\delta T\right| \tag{A6}$$

Based on the physical parameter tables and the experimental data, the maximum absolute and relative uncertainties of ρ, k, ρ_{in}, c_p, and v are identified as:

$$\delta\rho = 0.057\ \text{kg m}^{-3}, \delta\rho/\rho = 0.006\%;$$

$$\delta k = 3.5\times10^{-4}\ \text{W m}^{-1}\ \text{K}^{-1}, \delta k/k = 0.061\%;$$

$$\delta\rho_{in} = 0.05\ \text{kg m}^{-3}, \delta\rho_{in}/\rho_{in} = 0.005\%;$$

$$\delta c_p = 0.13\ \text{J kg}^{-1}\ \text{K}^{-1}, \delta c_p/c_p = 0.003\%;$$

$$\delta v = 0.007\times10^{-6}\ \text{m}^2\ \text{s}^{-1}, \delta v/v = 0.5\%.$$

Applying Eq. (A2) to Eqs. (2) and (3) (please refer to the manuscript), we can obtain the relative uncertainties of U_m and Re from (A7) and (A8), respectively.

$$\frac{\delta U_m}{U_m} = \left(\left(\frac{\delta V_{in}}{V_{in}}\right)^2 + \left(\frac{\delta\rho_{in}}{\rho_{in}}\right)^2 + \left(\frac{\delta\rho}{\rho}\right)^2\right)^{1/2} \tag{A7}$$

$$\frac{\delta Re}{Re} = \left(\left(\frac{\delta U_m}{U_m}\right)^2 + \left(\frac{\delta v}{v}\right)^2\right)^{1/2} \tag{A8}$$

where $\delta V_{in}/V_{in}$ is 1% based on the accuracy of the flow meter. Then, the relative uncertainties of U_m and Re are identified as: $\delta U_m/U_m$ = 1%, $\delta Re/Re$ = 1.1%. Similarly, the relative uncertainty of f is calculated as:

$$\frac{\delta f}{f} = \left(\left(\frac{\delta(\Delta p)}{\Delta p}\right)^2 + \left(\frac{\delta\rho}{\rho}\right)^2 + \left(2\frac{\delta U_m}{U_m}\right)^2\right)^{1/2} \tag{A9}$$

where $\delta(\Delta p)/(\Delta p)$ is 5% based on the accuracy of the pressure difference gauge. Then, the relative uncertainties of f are identified as: $\delta f/f$ = 5.4%.

The calculations for the uncertainty of Nu are deduced from (A10), (A11), (A12), (A13), (A14):

$$\frac{\delta Q}{Q} = \left(\left(\frac{\delta \rho_{in}}{\rho_{in}} \right)^2 + \left(\frac{\delta c_p}{c_p} \right)^2 + \left(\frac{\delta V_{in}}{V_{in}} \right)^2 + \left(\frac{\delta (T_{out} - T_{in})}{(T_{out} - T_{in})} \right)^2 \right)^{1/2}$$
$$= \left(\left(\frac{\delta \rho_{in}}{\rho_{in}} \right)^2 + \left(\frac{\delta c_p}{c_p} \right)^2 + \left(\frac{\delta V_{in}}{V_{in}} \right)^2 + \left(\frac{\delta T_{in}}{(T_{out} - T_{in})} \right)^2 + \left(\frac{\delta T_{out}}{(T_{out} - T_{in})} \right)^2 \right)^{1/2} \tag{A10}$$

The experimental minimum (T_{out}–T_{in}) is 9.1 °C and thus the maximum uncertainty of Q is identified as: $\delta Q/Q = 3.2\%$.

$$\frac{\delta(\Delta T)}{\Delta T} = \left((Err(T_{out} - T_{in}))^2 + \left(Err\left(In \frac{T_W - T_{in}}{T_W - T_{out}} \right) \right)^2 \right)^{1/2}$$
$$= \left(\frac{(\delta T_{in})^2 + (\delta T_{out})^2}{(T_{out} - T_{in})^2} + \left(\frac{1}{In \frac{T_W - T_{in}}{T_W - T_{out}}} Err\left(\frac{T_W - T_{in}}{T_W - T_{out}} \right) \right)^2 \right)^{1/2} \tag{A11}$$
$$\left(\frac{(\delta T_{in})^2 + (\delta T_{out})^2}{(T_{out} - T_{in})^2} + \frac{\left(\frac{(\delta T_W)^2 + (\delta T_{in})^2}{(T_W - T_{in})^2} + \frac{(\delta T_W)^2 + (\delta T_{out})^2}{(T_W - T_{out})^2} \right)}{\left(In \frac{T_W - T_{in}}{T_W - T_{out}} \right)^2} \right)^{1/2}$$

where $Err(F)$ means the relative uncertainty of function F. the maximum value of $\delta(\Delta T)/(\Delta T)$ is determined to be 3.7%.

$$\frac{\delta h}{h} = \left(\left(\frac{\delta Q}{Q} \right)^2 + \left(\frac{\delta(\Delta T)}{\Delta T} \right)^2 \right)^{1/2} \tag{A12}$$

$$\frac{\delta h_i}{h_i} = \left(\left(\frac{\delta h}{h}\right)^2 + \left(\frac{b \delta h}{1 - bh}\right)^2\right)^{1/2}$$
$$= \left(\left(\frac{\delta h}{h}\right)^2 + \left(\frac{bh}{1 - bh}\right)^2 \left(\frac{\delta h}{h}\right)^2\right)^{1/2} \tag{A13}$$

where $b = \frac{D_i}{2k_w} \ln \frac{D_o}{D_i}$ for the convenience of derivation. k_w is $42\ \mathrm{W\,m^{-1}\,K^{-1}}$ for the stainless steel and the maximum h is $5578\ \mathrm{W\,m^{-2}\,K^{-1}}$ in our experiment. Therefore, the relative uncertainty of h and h_i are identified as: $\delta h/h = 4.9\%$ and $\delta h_i/h_i = 5.1\%$.

$$\frac{\delta Nu}{Nu} = \left(\left(\frac{\delta h_i}{h_i} \right)^2 + \left(\frac{\delta k_i}{k_i} \right)^2 \right)^{1/2} \tag{A14}$$

Finally, the maximum uncertainty of Nu is identified as: $\delta Nu/Nu = 5.1\%$.

References

[1] A.E. Bergles, ExHFT for fourth generation heat transfer technology, Exp. Therm. Fluid Sci. 26 (2002) 335–344.
[2] A.E. Bergles, R.L. Webb, A guide to the literature on convective heat transfer augmentation, Adv. Enhanc. Heat Transfer, HTD 43 (1985) 81–89.
[3] A. Durmus, A. Durmus, M. Esen, Investigation of heat transfer and pressure drop in a concentric heat exchanger with snail entrance, Appl. Therm. Eng. 22 (2002) 321–332.
[4] R.M. Manglik, A.E. Bergles, Heat transfer and pressure drop correlations for twisted tape inserts in isothermal tubes: Part I – laminar flows, ASME J. Heat Transfer 115 (1993) 881–889.
[5] R.M. Manglik, A.E. Bergles, Heat transfer and pressure drop correlations for twisted tape inserts in isothermal tubes: Part II – transition and turbulent flows, ASME J. Heat Transfer 115 (1993) 890–896.
[6] X.Y. Zhang, Z.C. Liu, W. Liu, Numerical studies on heat transfer and flow characteristics for laminar flow in a tube with multiple regularly spaced twisted tapes, Int. J. Therm. Sci. 58 (2012) 157–167.
[7] P. Sivashanmugam, S. Suresh, Experimental studies on heat transfer and friction factor characteristics in laminar flow through a circular tube fitted with helical screw-tape inserts, J. Appl. Therm. Eng. 26 (2006) 1990–1997.
[8] P. Sivashanmugam, S. Suresh, Experimental studies on heat transfer and friction factor characteristics of turbulent flow through a circular tube fitted with helical screw-tape inserts, Chem. Eng. Process 46 (2007) 1292–1298.
[9] P. Promvonge, Thermal performance in circular tube fitted with coiled square wires, Energy Convers. Manage. 49 (2008) 980–987.
[10] A. Carcia, J.P. Solano, P.G. Vicente, A. Viedma, Enhancement of laminar and transitional flow in tubes by means of wire coil inserts, Int. J. Heat Mass Transfer 50 (2007) 3176–3189.
[11] K. Yakut, B. Sahin, The effects of vortex characteristics on performance of coiled wire turbulators used for heat transfer augmentation, Appl. Therm. Eng. 24 (2004) 2427–2438.
[12] A.W. Fan, J.J. Deng, A. Nakayama, W. Liu, Parametric study on turbulent heat transfer and flow characteristics in a circular tube fitted with louvered strip inserts, Int. J. Heat Mass Transfer 55 (2012) 5205–5213.
[13] S.O. Akansu, Heat transfers and pressure drops for porous-ring turbulators in a circular pipe, Appl. Energy 83 (2006) 280–298.
[14] Z.F. Huang, A. Nakayama, K. Yang, C. Yang, W. Liu, Enhancing heat transfer in the core flow by using porous medium insert in a tube, Int. J. Heat Mass Transfer 53 (2010) 1164–1174.
[15] K. Yakut, B. Sahin, Flow-induced vibration analysis of conical rings used for heat transfer enhancement in heat exchangers, Appl. Energy 78 (2004) 273–288.
[16] K. Yakut, B. Sahin, C. Celik, S. Canbazoglu, Performance and flow-induced vibration characteristics for conical-ring turbulators, Appl. Energy 79 (2004) 65–76.
[17] P. Promvonge, Heat transfer behaviors in round tube with conical ring inserts, Energy Convers. Manage. 49 (2008) 8–15.
[18] P. Promvonge, S. Eiamsa-ard, Heat transfer behaviors in a tube with combined conical-ring and twisted-tape insert, Int. Commun. Heat Mass Transfer 34 (2007) 849–859.
[19] S.K. Saha, U.N. Gaitonde, A.W. Date, Heat transfer and pressure drop characteristics of laminar flow in a circular tube fitted with regularly spaced twisted tape elements, Exp. Therm. Fluid Sci. 2 (1989) 310–322.
[20] S.K. Saha, A. Dutta, S.K. Dhal, Friction and heat transfer characteristics of laminar swirl flow through a circular tube fitted with regularly spaced twisted tape elements, Int. J. Heat Mass Transfer 44 (2001) 4211–4223.
[21] S. Eiamsa-ard, C. Thianpong, P. Promvonge, Experimental investigation of heat transfer and flow friction in a circular tube fitted with regularly spaced twisted tape elements, Int. Commun. Heat Mass Transfer 33 (2006) 1225–1233.
[22] Z.H. Ayub, S.F. Al-Fahed, The effect of gap width between horizontal tube and twisted tape on the pressure drop in turbulent water flow, Int. J. Heat Fluid Flow 14 (1993) 64–67.
[23] S. Eiamsa-ard, K. Wongcharee, S. Sripattanapipat, 3-D numerical simulation of swirling flow and convective heat transfer in a circular tube induced by means of loose-fit twisted tapes, Int. Commun. Heat Mass Transfer 36 (2009) 947–955.
[24] J. Guo, A.W. Fan, X.Y. Zhang, W. Liu, A numerical study on heat transfer and friction factor characteristics of laminar flow in a circular tube fitted with center-cleared twisted tape, Int. J. Therm. Sci. 50 (2010) 1263–1270.
[25] A.W. Fan, J.J. Deng, J. Guo, W. Liu, A numerical study on thermo-hydraulic characteristics of turbulent flow in a circular tube fitted with conical strip inserts, Appl. Therm. Eng. 31 (2011) 2819–2828.
[26] Y.H. You, A.W. Fan, W. Liu, S.Y. Huang, Thermo-hydraulic characteristics of laminar flow in an enhanced tube with conical strip inserts, Int. J. Therm. Sci. 61 (2012) 28–37.
[27] H.W. Coleman, W.G. Steele, Experimental and Uncertainty Analysis for Engineers, Wiley, New York, 1989.
[28] ANSI/ASME, Measurement Uncertainty, PTC 19.1-1985, 1986.
[29] R.L. Webb, Performance evaluation criteria for use of enhanced heat transfer surfaces in heat exchanger design, Int. J. Heat Mass Transfer 24 (1981) 715–726.